

**TECHNICAL REPORT**

**for NASA Grant NAG-2-541**

**NASA Technical Monitor: Alex Woo**

Grant Title: Development of 3D Electromagnetic Modeling Tools  
for Airborne Vehicles

Report Title: Progress on Hybrid Finite Element Methods for  
Scattering by Bodies of Revolution

Institution: Radiation Laboratory  
Department of Electrical Engineering  
and Computer Science  
The University of Michigan  
Ann Arbor MI 48109-2122

Period Covered: September 1991 – February 1992

Report Authors: J.D. Collins and J.L. Volakis

Principal Investigator: John L. Volakis  
Telephone: (313) 764-0500

# Progress on Hybrid Finite Element Methods for Scattering by Bodies of Revolution

Jeffery D. Collins and John L. Volakis

Radiation Laboratory  
Department of Electrical Engineering and Computer Science  
The University of Michigan  
Ann Arbor, Michigan 48109-2122

## Abstract

This report describes our progress on the development and implementation of hybrid finite element methods for scattering by bodies of revolution. It was found that our earlier finite element-boundary integral formulation suffered from convergence difficulties when applied to large and thin bodies of revolution. This report describes an alternative implementation where the finite element method is terminated with an absorbing termination boundary. In addition, an alternative finite element-boundary integral implementation is discussed for improving the convergence of the original code.

11/2/21

MR 0470

# 1 Introduction

A restraining factor in the numerical simulation of three-dimensional structures for electromagnetic scattering computations is the storage requirement associated with the chosen method. For sub-wavelength structures traditional methods [1] have been found to work well. However, for structures spanning several wavelengths, the storage requirement limits the use of these methods.

For the special case of axially symmetric structures or bodies of revolution (BOR), a reduction of the storage requirement is accomplished by reducing the three-dimensional problem to a set of two-dimensional ones. Several moment method codes have been developed for the solution of these ([2] - [7] and others). However, for large structures the required storage of  $O(N^2)$ , where  $N$  denotes the number of unknowns over the BOR cross section, limits their use.

To further reduce the storage requirement, hybrid finite element methods ([8]-[12], etc.) may be used, since the storage associated with the finite element method is  $O(N)$  in contrast to the  $O(N^2)$  requirement of moment methods. These methods differ from one another primarily by the application of the radiation condition. The most accurate method enforces the radiation implicitly through an application of the boundary integral equation (BI) over a fictitious boundary enclosure. By nature of the full matrix encountered over the enclosure, this method is one of a class of boundary conditions referred to as “global” boundary conditions. A reduction in storage is realized by choosing a fictitious enclosure in the shape of a circular cylinder on which some of the integrals become convolutional and may thus be evaluated with the FFT in conjunction with an iterative solver [13]. Less accurate but more efficient methods of storage involve the use of “local” boundary conditions, the most typical

of which being the absorbing boundary condition (ABC) [14]. Another local condition involves the application of a simple first order condition (i.e., Dirichlet or impedance) on the exterior boundary immediately adjacent to multiple absorbing material layers that are included in the solution of interior problem [15]. This is termed the artificial termination boundary (ATB).

For all hybrid finite element methods formulations mentioned above, the finite element (FE) system is formed by discretizing the coupled potential equations [10] via the usual finite element method. The resulting system is then augmented by either a discrete representation of the Stratton-Chu equations [16] for the boundary integral approach, a discrete version of the ABC's [18] or the free space impedance boundary condition (adjacent to absorbing layers) for the ATB approach.

In this report, we present the current status of this research. Each section considers a different hybrid finite element method and discusses our progress on that method.

## **2 Finite element – boundary integral method**

A finite element – boundary integral method for the scattering by bodies of revolution was previously developed [13]. In that report, the structures studied were restricted to sizes  $O(1\lambda)$  due to inaccuracies in the BI subsystem. (It was originally thought that since the finite element portion had inaccuracies in the vicinity of the singular shell of radius  $k_0\rho = m$ , it must be the source of the inaccuracies. But after separating the BI and FE subsystems that the source of the problem was revealed. It should be noted that tests performed on the FE system using the incident field as the boundary condition to a free space solution region, validated the FE subsystem.)

Enforcing the pec boundary conditions on the BI system (each unique term of the original BI subsystem preserved), scattering tests were performed on ogives of normalized size  $1\lambda \times 0.088\lambda$  for axial incidence. The current produced from this system is highly oscillatory in the  $J_\phi$  component (denoted  $J_p$  in the figures), whereas the  $J_t$  component is virtually unaffected in comparison to the Method of Moments (MoM) [17]. This is seen in Figs. 1 – 4 for a  $3\lambda$  and a  $10\lambda$  version of the ogive, respectively. To correct this problem, the suspect portion of the system was weighted with linear weighting functions, instead of pulse functions, as was used in the original formulation. This resulted a much smoother currents, as indicated in the Figs. 1 and 2. Note, however, that as the structure becomes large, inaccuracies near  $k_0\rho = m = 1$  (corresponding to index positions 12 and 50 in Figs. 1 and 2 and indices 12 and 195 in Figs. 3 and 4) become even larger, particularly for the  $10\lambda$  ogive. This translates to correspondingly large errors in the far fields, which are more apparent in the backscatter and forward scatter regions. After a careful re-evaluation of the self-cell terms in the formulation, the problem continued to exist. The source of the problem was then deduced to be the inaccurate matrix element evaluations near the observation cell, since some of the integrands are strongly singular. This, as well as extending all weighting and basis functions to linear form will be considered in a future work.

### **3 Elimination of internal resonances from the FE-BI system**

We have recently found for two dimensional problems [19] that the use of the scattered field formulation eliminates the resonance problem associated with the boundary integral portion of the formulation. We are currently investigating the reason behind this. Additionally, a method involving the use of a complex wave number in place of the usual free space

wave number for the same purpose will be implemented. The authors of [20] indicate an improved condition number (important for fast CG convergence) and excellent results for a two dimensional example. We have experienced the same through some limited testing.

## 4 Finite element – artificial termination boundary method

The finite element development of the previous section was modified for a scattered field implementation. To ensure the outgoing nature of the wave, our ATB was used. This absorber was developed by minimizing the reflection coefficients from an impedance backed three material layer absorber ( $\epsilon_{r1} = 0.3801 + j0.3098$ ,  $\epsilon_{r2} = 3.2211 + j1.3129$ ,  $\epsilon_{r3} = 2.2448 + j0.6698$ ,  $\mu_{ri} = \epsilon_{ri}$ , each has thickness  $\tau = 0.055\lambda$  and are numbered from innermost to outermost). Assuming that deforming this planar absorber into a spherical shape (or any other shape) preserves its absorbing characteristics, the finite element region was be terminated at some distance from the scatterer.

To determine the absorbing qualities of the spherically shaped absorber, tests were performed by placing an x-directed electric dipole source inside a fictitious spherical boundary as indicated in Figs. 5 and 6. The absorbing layers were placed at a minimum distance of  $\lambda/2$  from the inner boundary in Fig. 5 and  $1\lambda$  in Fig. 6. Enforcing the Dirichlet boundary condition for the electric field and the Neumann condition for the magnetic field (as would be the case for a perfect conductor on the same boundary), the position of the dipole was varied from the center of the sphere along the axis of revolution to a distance  $\lambda/4$  from the inner boundary as indicated in Fig. 5. (The inner boundary was chosen as such to reduce the number of unknowns required for the test. This was also necessary because of the strong singular nature of the source.) Fig. 7 displays the far  $H_\phi$  field patterns (the  $\phi = 0$  cut) of the dipole as computed by integrating along the surface of the inner sphere and after

solving the system for those fields via the FE-ATB method. A comparison is made with the exact results. For a source position  $z_0 = 1\lambda$ , the far field pattern begins to deviate by approximately 1 dB. For an axial position of  $z_0 = 1.25\lambda$  significant deviation has occurred. At this point, the source is  $1.5\lambda$  from the innermost layer of the absorber. Thus, a scatterer would have to be at least this distance from this absorber to obtain reasonable results.

Scattering patterns for spheres of  $1\lambda$  and  $1.5\lambda$  using the same absorber geometry are found in Figs. 8 – 10. Clearly, the results of the smaller sphere are better, but because of multiple interactions with the absorbing layers, oscillations in the pattern are still produced. In order to obtain better results, better absorbers must be designed. A temporary alternative is the use of the standard absorbing boundary conditions, described in the next section.

## **5 Finite element – absorbing boundary condition method**

The mesh may be terminated by the use of the standard ABCs [18] for the body of revolution. This is currently under development. The code is being modified to allow for general form higher order boundary conditions to be developed in the future, which conform to the scattering body.

## **6 Summary**

We have presented a summary of the work performed during the past year. Work currently in progress and expected to be completed soon is itemized as follows:

- Modify the BI subsystem for better accuracy and stability



- Resolve the resonance problem by either the scattered field approach or via the complex wave number approach
- Couple the ABCs to the FE subsystem
- Modify the FE subsystem to include resistive cards and impedance boundary conditions
- Perform a study on multilayered radome structures

The details of the previous work in addition to that mentioned above will be available in a full report at the end of March.

## References

- [1] S.M. Rao, D.R. Wilton and A.W. Glisson, "Electromagnetic scattering by surfaces of arbitrary shape," *IEEE Trans. Antennas Propagat.*, vol. AP-30, pp. 409-418, 1982.
- [2] M.G. Andreasen, "Scattering from bodies of revolution," *IEEE Trans. Antennas Propagat.*, pp. 303-310, March 1965.
- [3] J.R. Mautz and R.F. Harrington, "Radiation and scattering from bodies of revolution," *App. Sci. Res.*, pp. 405-435, June 1969.
- [4] T.K. Wu and L.L. Tsai, "Scattering from arbitrarily-shaped dielectric bodies of revolution," *Wave Motion*, vol. 12, pp. 709-718, Sep.-Oct. 1977.
- [5] A.W. Glisson and D.R. Wilton, "Simple and efficient numerical techniques for treating bodies of revolution," The University of Mississippi Tech. Rept. No. 105, March 1979.
- [6] A.W. Glisson, D. Kajfez and J. James, "Evaluation of modes in dielectric resonators using a surface integral equation formulation," *IEEE Trans. Microwave Theory Tech.*, vol. MTT-31, pp. 1023-1029, Dec. 1983.
- [7] J.M. Putnam and L.N. Medgyesi-Mitschang, "Combined field integral equation formulation for axially inhomogeneous bodies of revolution," *McDonnell Douglas Research Laboratories report QA003*, Dec 1987.
- [8] B.H. McDonald and A. Wexler, "Finite-element solution of unbounded field problems," *IEEE Trans. Microwave Theory Tech.*, vol. MTT-20, pp. 841-847, Dec. 1972.
- [9] K.K. Mei, "Unimoment method of solving antenna and scattering problems," *IEEE Trans. Antennas Prop.*, vol AP-22, pp. 760-766, Nov. 1974.

- [10] M.A. Morgan, S.K. Chang and K.K. Mei, "Coupled azimuthal potentials for electromagnetic field problems in inhomogeneous axially symmetric media," *IEEE Trans. Antennas Propagat.*, pp. 413-417, May 1977.
- [11] Jian-Ming Jin and Valdis V. Liepa, "Application of hybrid finite element method to electromagnetic scattering from coated cylinders," *IEEE Trans. Antennas Propagat.*, vol. AP-36, pp. 50-54, Jan. 1988.
- [12] S.-Y. Lee, "Highly storage-efficient hybrid finite element/boundary element method for electromagnetic scattering," *Electronic Letters*, vol. 25, pp. 1273-1274.
- [13] J.D. Collins and J.L. Volakis, "A combined finite element – boundary element formulation for solution of axially symmetric bodies," Rad. Lab. Report # 025921-18-T, The University of Michigan, 1991.
- [14] A. Bayliss, M. Gunzburger and E. Turkel, "Boundary conditions for the numerical solution of elliptic equations in exterior regions," *Siam J. Appl. Math.*, vol. 42, no. 2, pp. 430-451, April 1982.
- [15] J.M. Jin, J.L. Volakis and V.V. Liepa, "An engineer's approach for terminating finite element meshes in scattering analysis," 1991 AP-S Symposium Digest, pp. 1216–1219.
- [16] J.A. Stratton, *Electromagnetic Theory*, New York: McGraw-Hill, 1941.
- [17] J.R. Mautz and R.F. Harrington, "An improved E-field solution for a conducting body of revolution," *Technical Report TR-80-1*, Syracuse University, 1980.
- [18] A. F. Peterson, "Absorbing boundary conditions for the vector wave equation," *Microwave and Optical Tech. Letters*, vol. 1, pp. 62-64, April 1988.

- [19] J.D. Collins, J.M. Jin and J.L. Volakis, "A combined finite element - boundary element formulation for solution of two-dimensional problems via CGFFT," *Electromagnetics*, Dec 1991.
- [20] W.D. Murphy, V. Rokhlin and M.S. Vassiliou, "Solving electromagnetic scattering problems at resonance frequencies," *J. Appl. Phys.*, vol. 67, pp. 6061-6065, May 1990.

## List of Figures

1	The $J_t$ current on a $3\lambda$ ogive. . . . .	11
2	The $J_\phi$ current on a $3\lambda$ ogive. . . . .	11
3	The $J_t$ current on a $10\lambda$ ogive. . . . .	12
4	The $J_\phi$ current on a $10\lambda$ ogive. . . . .	12
5	Mesh for a $1.5\lambda$ sphere inside an absorbing spherical enclosure, the various layers of which are indicated by the shading. . . . .	13
6	Mesh for a $1\lambda$ sphere inside an absorbing spherical enclosure, the various layers of which are indicated by the shading. . . . .	14
7	$H_\phi$ scattering patterns for an x-directed electric dipole for various source positions along the axis of revolution. . . . .	15
8	$TE_z$ scattering pattern for a $1.5\lambda$ conducting sphere. . . . .	16
9	$TE_z$ scattering pattern for a $1\lambda$ conducting sphere. . . . .	17
10	$TM_z$ scattering pattern for a $1\lambda$ conducting sphere. . . . .	17

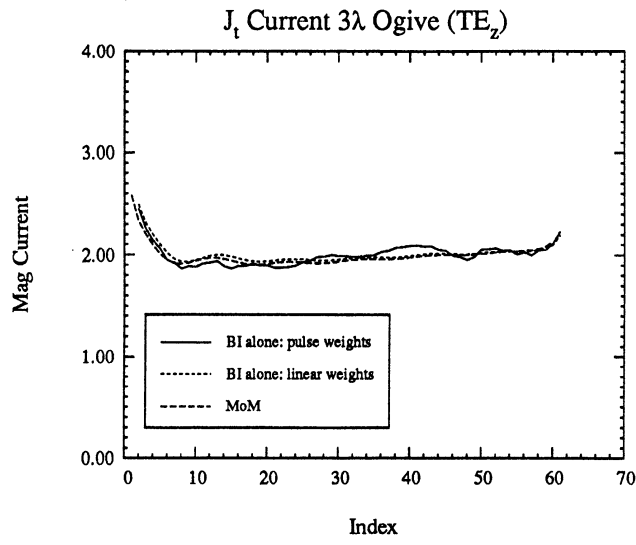


Figure 1: The  $J_t$  current on a  $3\lambda$  ogive.

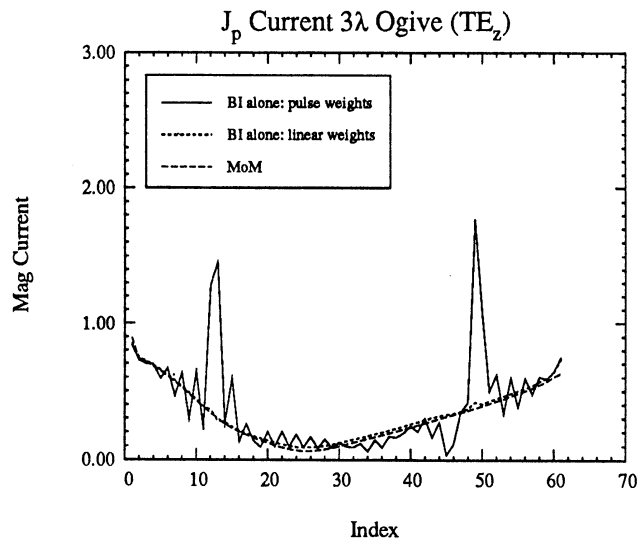


Figure 2: The  $J_\phi$  current on a  $3\lambda$  ogive.

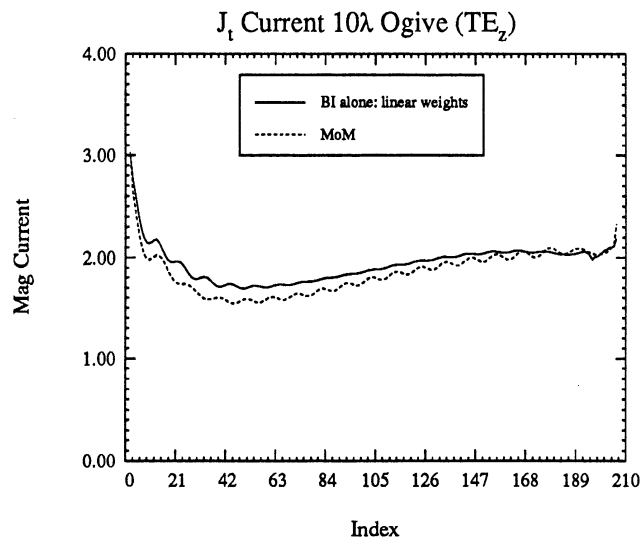


Figure 3: The  $J_t$  current on a  $10\lambda$  ogive.

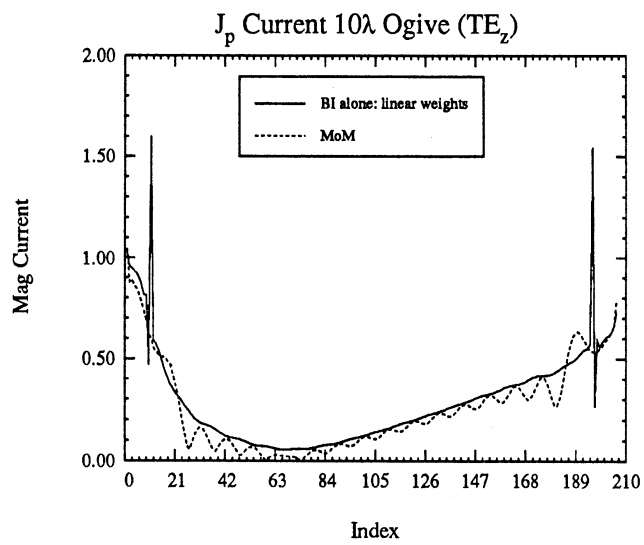


Figure 4: The  $J_\phi$  current on a  $10\lambda$  ogive.

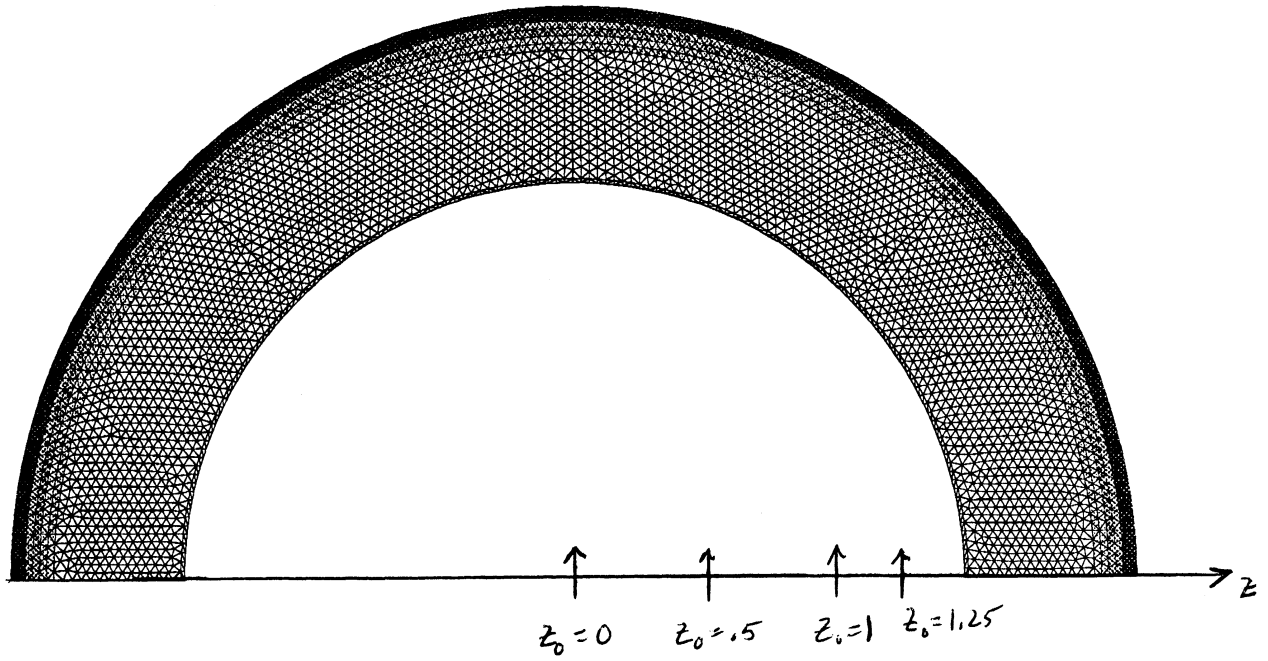


Figure 5: Mesh for a  $1.5\lambda$  sphere inside an absorbing spherical enclosure, the various layers of which are indicated by the shading.



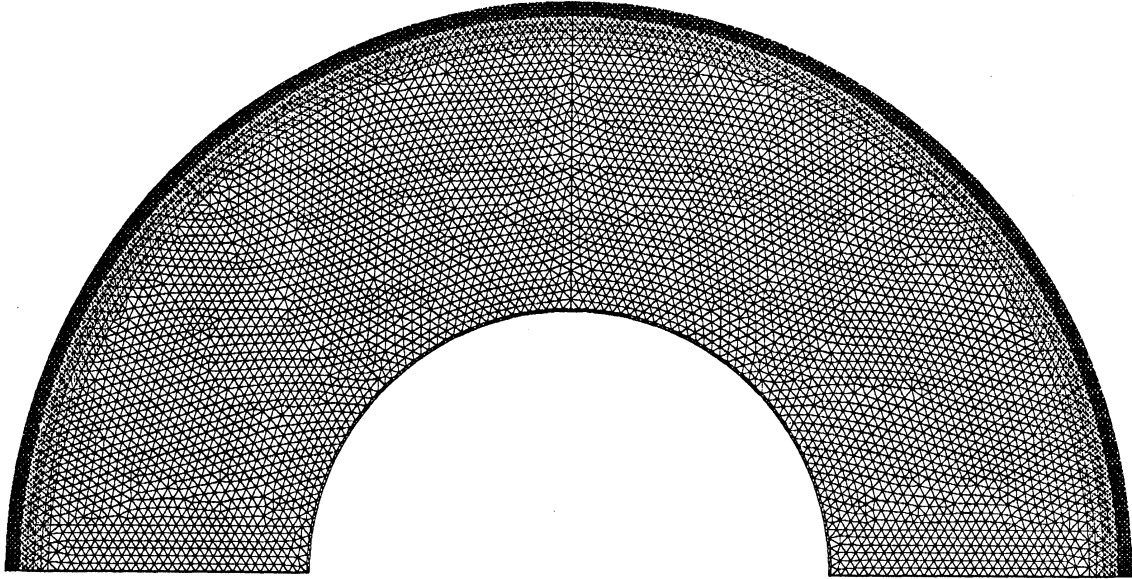


Figure 6: Mesh for a  $1\lambda$  sphere inside an absorbing spherical enclosure, the various layers of which are indicated by the shading.

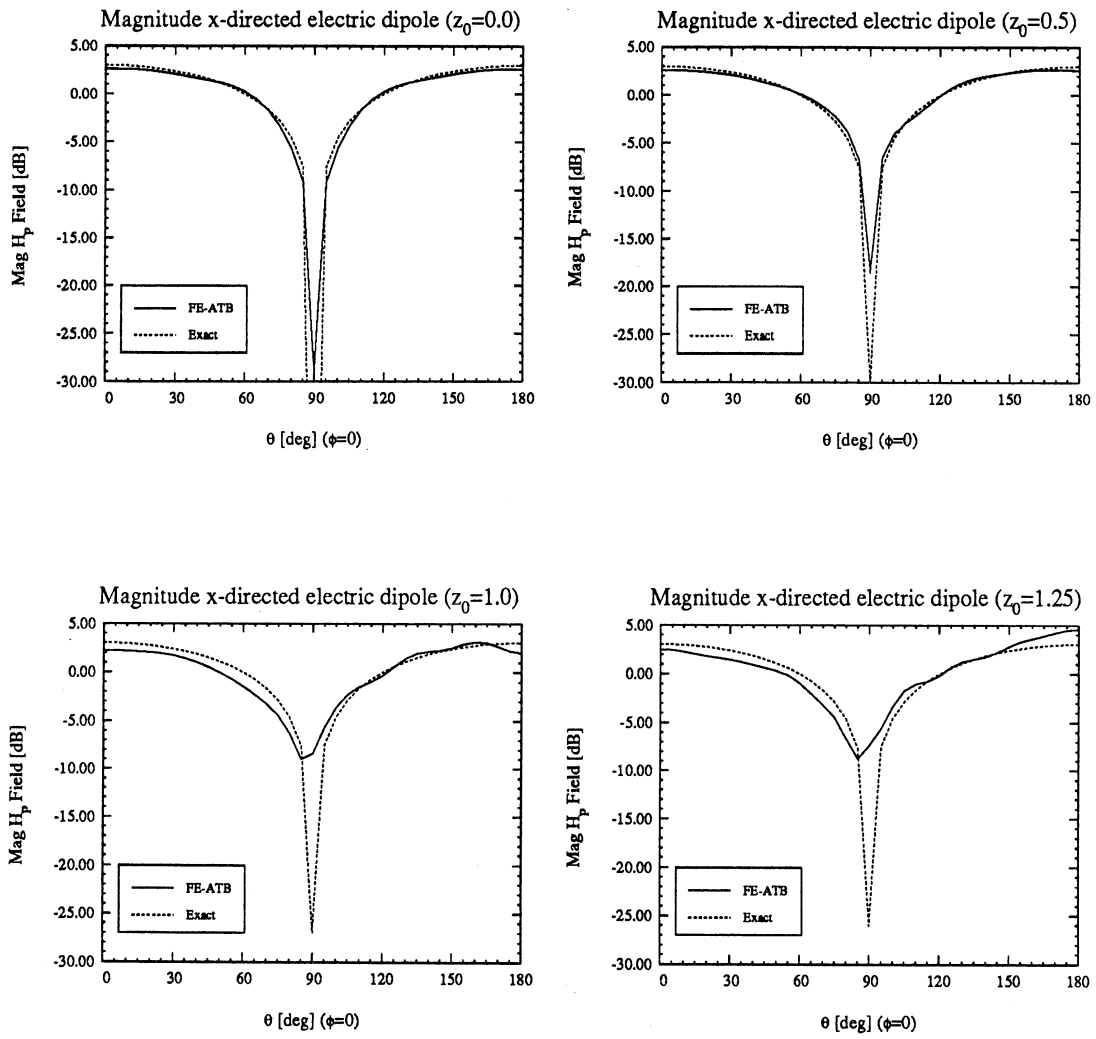


Figure 7:  $H_\phi$  scattering patterns for an x-directed electric dipole for various source positions along the axis of revolution.

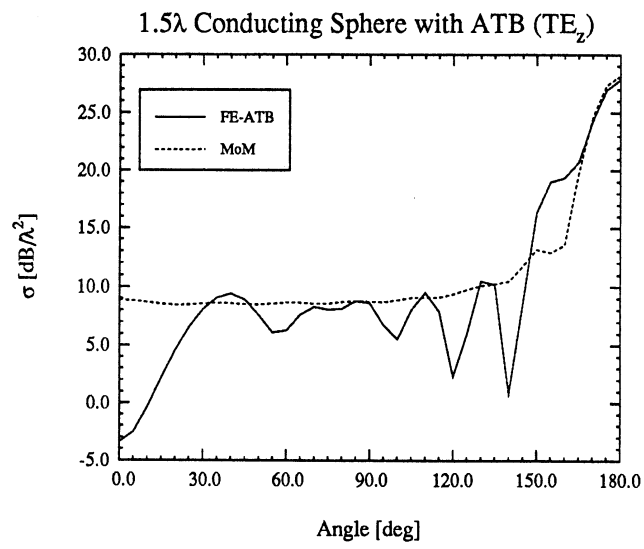


Figure 8:  $TE_z$  scattering pattern for a  $1.5\lambda$  conducting sphere.

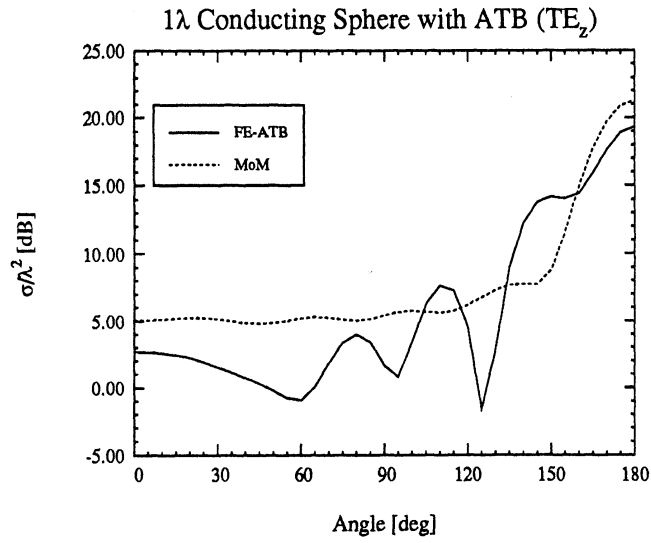


Figure 9:  $TE_z$  scattering pattern for a  $1\lambda$  conducting sphere.

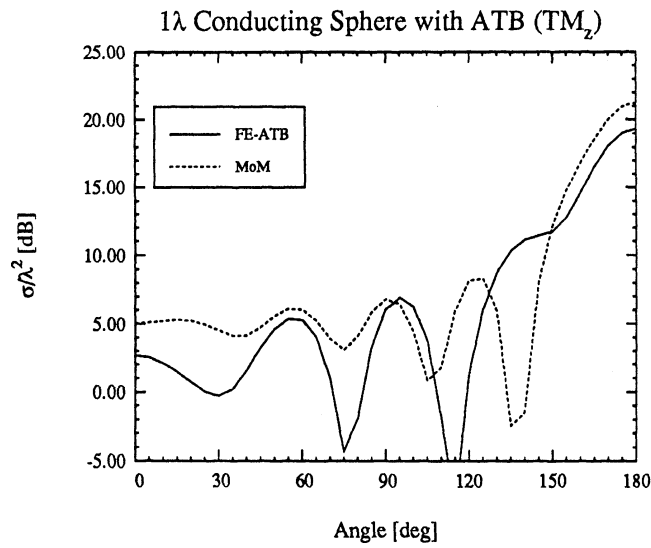


Figure 10:  $TM_z$  scattering pattern for a  $1\lambda$  conducting sphere.



3 9015 02229 1721

THE UNIVERSITY OF MICHIGAN

DATE DUE

7/10 6:02p